Investigation of cycloaliphatic amine-cured bisphenol-A epoxy resin under quenching treatment and the effect on its carbon fiber composite lamination strength

Naga Sai Prasad[1*], Deepak Kumar Sethy[2]

[1*]Associate Professor, Department of Mechanical Engineering, Nalanda Institute of Technology, Bhubaneswar, Odisha, India
[2]Assistant Professor, Department of Mechanical Engineering, Nalanda Institute of Technology, Bhubaneswar, Odisha, India

*Corresponding author e-mail: nagasaiprasad@thenalanda.com

Abstract: Thermosetting epoxy resin polymer with cycloaliphatic amines curing agent has been widely used for a composite matrix with carbon fiber reinforcement. The utilization was increased due to the superior performance of this epoxy resin compared to other polymers. However, a changing operational environment has potentially reduced composite performance, which most likely begins with matrix degradation. This research applies thermal treatment by the quenching process sequence to the epoxy resin matrix and its reinforced carbon fiber composite (CFRP). The composite is made by epoxy resin diglycidyl ether bisphenol-A, curing with cycloaliphatic amine as matrix and strengthening carbon fiber mat/woven. Three times quenching treatment was performed by heating the specimen around the glass transition temperature and then dipped immediately in fresh water. After quenching treatment, the epoxy resin shows a reduction in tensile strength and elongation. Under infrared observation, epoxy resin does not significantly show changes in functional groups. Investigation under X-ray refraction also indicates no difference in a crystalline structure; this epoxy resin stays in an amorphous form before and after quenching. In contrast to the matrix, the quenching treatment of the CFRP composite above the epoxy resins glass transition temperature revealed an increase in the inter laminar shear strength (ILSS). The matrix ductility reduction after quenching should be carefully considered for application in the form of epoxy resin sheets or CFRP composite construction materials.

Keywords: cycloaliphatic amine, inter laminar shear strength,quenching, fiber carbon mat

1 Introduction

The diglycidyl ether of bisphenol-A (DGEBA) epoxy resin is a thermoset polymer that has been widely used as a composite matrix for construction materials. Its advantages and unique properties lead to an increase in the consumption of this material. For example, epoxy resins can be reinforced with carbon fibers to produce composite materials called carbon fiber-reinforced polymer composites (CFRP). These composites are strong, lightweight, malleable, and highly resistant to corrosion, water, and fatigue [1]. Applications of CFRP composites are found in aircraft components, ship construction, automotive, civil buildings, sports equipment, and households [2,3]. Many survey results predicted that construction engineers would reduce the use of metal materials and switch to CFRP materials in the future. This prediction has the consequence of increasing the consumption of carbon fiber and epoxy resin by about 12% annually [4]. In addition, most thermoset epoxy resins are cured using an amine hardener or curing agent. The epoxy resin system developed by the hardener can withstand high temperatures and is considered a suitable matrix in struc- tural composites [5]. Cycloaliphatic amines, one of the variants of amine hardeners, have specific characteristics as a combination of the properties of aliphatic and aromatic amines. This amine can form a robust tertiary amine cross linked network at the end of curing [6]. The composition of this epoxy resin system also does not have a negative impact on the mechanical and chemical properties [7], with a curing time that is technically andeconomically acceptable [8].

As a construction material, CFRP is often used in places that are directly exposed to the environment. Sudden and extreme environmental changes play a role as dynamic loads on CFRP composites that have the poten-tial to cause structural failure. For example, thermal shock can cause internal stresses due to material expansion and contraction during heating and cooling treatments or differences in the coefficients of thermal expansion of composite material components [9]. Epoxy resins also experience dimensional deviation when heated and cooled at the same rate [10]. However, epoxy resins generally maintain their tensile strength and modulus of elasticity up to 200°C [11]. Carbon fiber and thermosetting polymer matrices in CFRP composites significantly differ in the thermal expansion coefficient. Microscopically they have the potential to cause interfacial stress due to differences in deformation rates when subjected to thermal loads [12]. The distinction of deformation rate between the fiber and the matrix initiates the breakdown of cross-links and forms a stress concentration at the interface [13]. Heating and cooling affect composites' tensile strength and impact due to two aspects. First, the difference in the coefficient of thermal expansion of the fiber and the epoxy resin forms deformation, micro-cracks, and tension or compression at the interface. Second, post-curing at high temperature increases cross-linking at the interface and strengthens the impact strength [14]. One of the two aspects that is more dominant will contribute greatly in determining the composite properties.

This article describes the changes in epoxy resin and CFRP characteristics after thermal loading through a quenching treatment subjected to up to three cycles. Rapid temperature changes in the quenching process can potentially change the epoxy resin's molecular bonds and functional groups. In addition, exposure to high tem-peratures and immersion in water within an atmospheric environment can affect the tensile strength and elonga- tion of the epoxy resin. Furthermore, the laminar bond between the epoxy resin matrix and the carbon fiber mat is likely to be different when water molecules have the opportunity to penetrate the composite structure.

2 Materials

The CFRP composite matrix is made of epoxy resin bisphenol A epichlorohydrin (DGEBA, brand: Eposchon) with an epoxide function of 189 ± 5 and cycloaliphatic amine (brand: Eposchon EP 555) for the hardener containing 3-aminomethyl-3,5,5 trimethylcyclo-hexylamine. Based on the constituent function groups, this hardener is categorized as isophorone diamine [15], which has a hydrogen equivalent weight of 86 and a viscosity of 0.05–0.1 N s/m2 at room temperature [16]. The CFRP composite reinforcement uses a carbon fiber mat (brand: Toray, type: T300). This mat is woven by a 2×2 twill and plain pattern with five yarns every 10 mm distance. Each yarn consists of 3,000 fiber filaments, which results in a density of 200 g/m2 with an average thickness of 0.2 mm. The detailed properties of carbon fiber are shown in Table 1. Before being used, epoxy resin and carbon fiber are not sub- ject to pre-treatment (as received).

3 Methods

Epoxy resin and hardener with a ratio of 2/1 were mixed carefully and homogeneously to produce the epoxy resin matrix. The curing time in the atmosphere was set for a minimum of 42 h. The next step, post-curing within the programmable electric oven, was performed at a tem-perature of 60°C for 6 h [17]. The final shape of the epoxy resin matrix was a sheet or board with an average thick- ness of 2 mm. A similar procedure was adopted for com- posing the CFRP composite in which the carbon fiber mat was placed exactly in the middle of the matrix thickness.

Table 1: The properties of the carbon fiber used in this research (concerning the datasheet issued by Toray Composite Materials, Inc.)

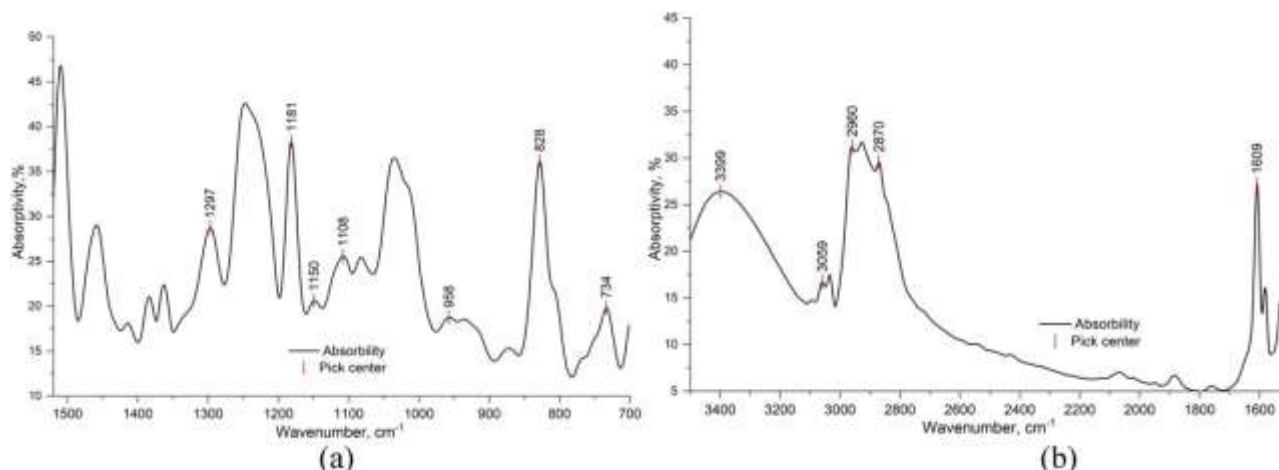| Property	Value	Property	Value
Tensile strength	3.53 GPa	Coefficient thermal expansion	$-0.41 \times 10^{-6}/°C$
Tensile modulus	230 GPa	Specific heat	0.777 J/g °C
Strain at failure	1.5%	Thermal conductivity	0.105 J/cm s °C
Density	1.76 g/cm^3	Electric resistivity	$1.7 \times 10^{-3} \Omega$ cm
Filament diameter	7 µm	Chemical composition	Carbon >93%
Yield	198 g/1,000 m	Impurities	<50 ppm

Figure 1: Infrared spectrum zones of (a) fingerprint and (b) overtone of epoxy resin specimen without quenching treatment.

Figure 1 depicts a fully cured epoxy resin's infrared spectrum (Fourier transformation infrared, FTIR). The functional group determination of each wavenumber peak is listed in Table 2. Spectrum tracing in the fingerprint region (500 until 1,500/cm), a double bond zone (1,500 until 2,000/cm), a triple bond zone (2,000 until 2,500/cm), and single bond (2,500 until 4,000/cm) are the pattern or character of the spectrum of thermosetting polymeric materials [18]. The epoxy functional group was detected at the wavenumber peak of 828, 958, 1,181, 1,297, 1,609, and 2,927/cm [19].

Figure 2 is a differential scanning calorimeter (DSC) curve resulting from epoxy resin thermal testing with a heating rate of 10°C/min. The DSC curve confirmed that epoxy resin's glass transition temperature (T_g) is 131°C, with on-site and off-site points at 61 and 201°C, respectively. The peak of the first curve at 270°C with energy of 47,537 J/g shows the crosslink network formation of epoxy resin. The second curve peak at 515°C shows the burning emerging of the aromatic epoxy resin function, producing heat equal to 295,231 J/g.

In the next step, the epoxy resin matrix specimen and CFRP composite were subjected to quenching treat-ment at a target temperature of 125 and 150°C and cooling media of aquades at room temperature (25°C).

First, the heating process was conducted in the programmable electric oven, where the temperature was gradually raised at the rate of 25°C/min. When the temperature reached the target, it was held for 3 minutes to ensure temperature uniformity in all segments of the specimen. Second, the sample was immediately immersed in a container filled with aquades. Its volume must ensure no increasing temperature after the specimen is immersed. The second and third quenching are repetitions of the treatment above after the sample is immersed in water for at least 5 min.

For testing purposes, the specimens were conditioned according to the test standard and identified by code, as shown in Table 3. The molecular network and crystal structure were tested with FTIR and XRD, respectively. Investigation of changes in mechanical properties of the epoxy resin was conducted by tensile test according

Table 2: Thermoset epoxy resin functional groups detected as infrared wavenumber peaks by FTIR (assignment refers to Coates [20])

| Wavenumber peak (1/cm)	Group of Wavenumber (1/cm)	Origin bonding	Functional group/assignment
734	720–750	{–CH₂–}	Methylene/saturated aliphatic (alkane/alkyl)
828	820–890	{C–O–O}	Epoxy and oxirane ring/ether and oxy compound
958	925–1,005	{▮CH₂}	Methylene/saturated aliphatic (alkane/alkyl)
1,108	1,070–1,140	{C–O–C}	Cyclic ether/ether and oxy compound
1,181	1,130–1,190	{C–N}	Secondary amine/amine and Amino compound
1,297	1,280–1,350	{C–N}	Aromatic amine/amine and amino compound
1,609	1,580–1,615	{C▮C–C}	The aromatic ring (aryl)
2,870	2,860–2,880	{–CH₃}	Methyl/saturated aliphatic (alkane/alkyl)
2,960	2,950–2,970	{–CH₃}	Methyl/saturated aliphatic (alkane/alkyl)
3,029	3,010–3,040	{C–H}	Olefinic (alkene)
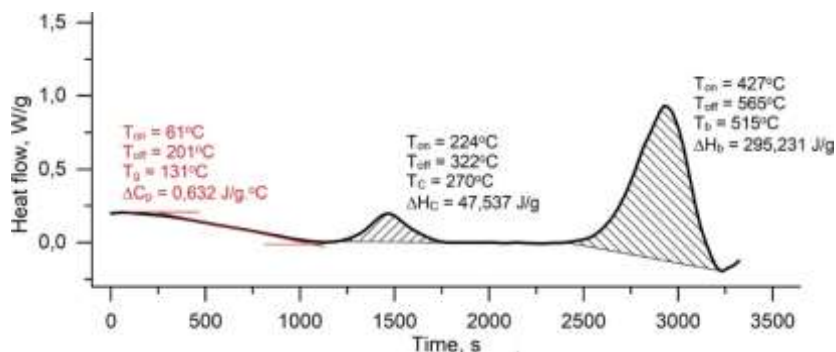
Figure 2: DSC curve of epoxy resin specimen without quenching.

to ASTM D638-14 [21]. In comparison, the quality bonding of the composite was mechanically tested with the short beam bending method to determine the shear strength of its interfacial bond. This test refers to the ASTM D2344-2003 [22] with the average width and thickness of CFRP composite of 11.463 and 1.898 mm, respectively. Regarding this composite thickness, the supporting points were set at a distance of 10,880 mm to meet the requirements of the test standard. The data were statistically analyzed from five specimens to get the average value and coefficient of variation (CV).

4 Results

X-ray diffraction and infrared spectrum of epoxy resin

Figure 3: X-ray spectrum of the specimen before and after quenching treatment.

The quenching treatment did not cause the crystal struc- ture formation in the epoxy resin. As shown in Figure 3, the epoxy resin formed until the end of the curing process produces a pure amorphous material. Similar X-ray dif- fraction was also obtained for the amorphous polyur- ethane material [23]. The quenching treatment up to three times with the target temperature above T_g also did not show the formation of a crystalline structure. The peak formed at an incidence angle of $2\theta = 18°$ is proven to be very gentle, indicating no appearance of a crystalline structure [24]. In general, sharp impulses at

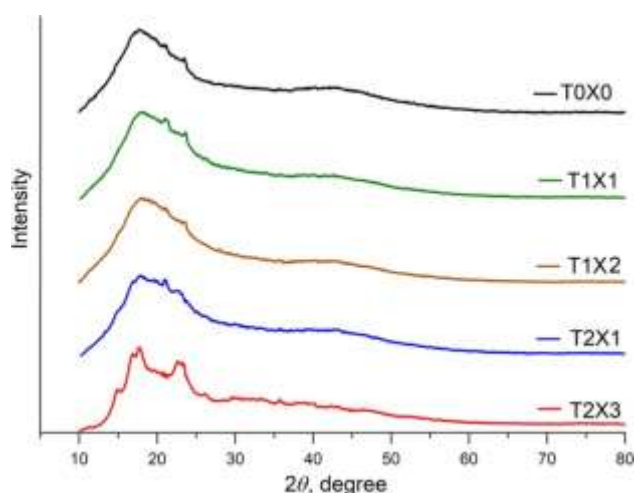the X-ray intensity peak that indicate the crystal struc- ture's presence do not appear along the diffraction angle interval. This fact suggests that the release of thermal energy by the epoxy resin during the quenching process is insufficient to convert the crosslinked network or other phases into nucleation to form a crystalline struc- ture [25].

In the absence of a crystal structure, a crosslinked network plays a very dominant role in determining the properties of epoxy resin. Figure 4 shows the infrared spectrum of the quenched epoxy resin. There is no new absorptivity peak overall wavenumber that indicates no

Table 3: Specimen identification for testing

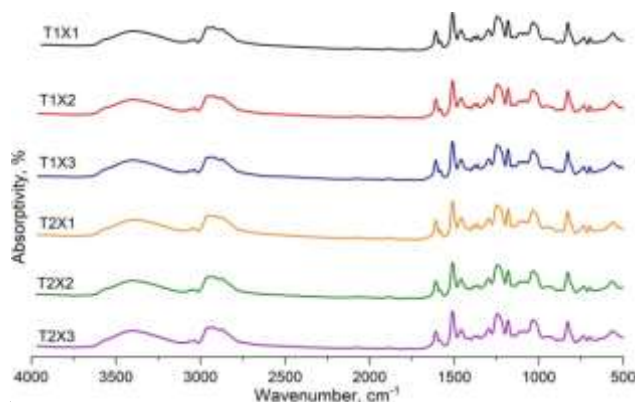| Specimen designated	T0X0	T1X1	T1X2	T1X3	T2X1	T2X2	T2X3
Temperature target (°C)	No treatment	125	125	125	150	150	150
Number of quenching		1	2	3	1	2	3

Figure 4: Infrared spectrum of the specimen after quenching with various conditions.

functional group created after quenching. However, the infrared spectrum shows a crosslinked network that forms secondary or tertiary amine groups with C–H_2, N–H, and –CH_3 main bonds [26]. C–H_2 and C–H_3 bonds were detected by infrared at wavenumber 2,970–2,860/cm and N–H wag bonds at wavenumber 733/cm. The C–N crosslinks in secondary amines were found at wavenumber 1,149/cm [27]. The crosslink is also formed through the reaction between the epoxy groups, creating a cyclic ether group characterized by the presence of C–O–C bonds at the infrared spectrum wavelength 1,108/cm [28]. The invisible peak of 915/cm in the infrared spectrum indicates that the epoxy ring is in the open state. The absence of this peak was detected after the epoxy resin system was sub-jected to post-curing treatment, as shown in Figure 1. This condition confirms the impossibility of changing the crosslinking structure naturally due to the unavail-ability of an epoxide molecule to be combined with the hardener amine group. However, the crosslink density can be improved through vitrification or etherification mechanism by adding heat that is sufficient to drive the molecular movement [29]. The broad spectrum between 3,500 and 2,500/cm strongly shows the bonding region of the O–H atoms in the carboxylic functional group. The spectrum of wavenumber 1,182/cm is a character for C–N bonds that experience stretching vibration when exposed to infrared light. The loss of intensity in the epoxy ring groups and the presence of O–H and C–N groups confirmed the conversion of the epoxy groups into polymer chains and crosslink networks [30].

Epoxy group conversion might be analyzed by comparing a specific wavenumber's function group peak area. The conversion could be predicted *via* the car-boxylic group peak area (at 3,059/cm) and the DGEBA ring (at 1,108/cm) as reference [31]. It was also allowed

to calculate it involving the peak area of the oxirane function group at 823–847/cm and taking a reference group of the aromatic ring at 733 or 1,586/cm [32]. The other way, the C–O bond of the oxirane ring at 1,131/cm, which it opens when reacting with the amine group, and the reference area of the aromatic ring peak at 1,603/cm can also be used as an alternative for calculating the conversion of the epoxide group [33]. Epoxy extension reaction equation or functional group conversion is most commonly used to calculate the degree of crosslinking of epoxy resins during curing [34], as follows:

$$R_{ij} = \left(\frac{(A_f/A_r)_t}{(A_f/A_r)_0} \right)_t .$$

The subscripts i and j represent the temperature and the number of quenching cycles, respectively. The nota-tions A_f and A_r are the functional group peak area and the reference peak area, respectively. The subscript 0 is used as the condition of the unquenched specimen, and t to indicate the state of the sample subjected to the quenching process.

The calculation of the epoxy extension reaction resulted in a change in the number of crosslinked chains that occurred in the specimen after quenching treatment. Peak area changes in the infrared spectrum at 828 and 3,059/cm were used as the basic conversion of the functional groups of the epoxy resin regarding wavenumbers 733 and 1,108/cm, respectively. Figure 5 shows the patterns of peak area at the wavenumber for conversion analysis of epoxy crosslink. Table 4 contains the calculation results of the conversion of epoxy functional groups, which offer a tendency to decrease the number of crosslinked networks when repeated quenching treatment. However, the effect of quenching temperature did not show a significant difference in the number of crosslinks. The crosslink formation process for the vitrified epoxy-amine resin system at 100°C takes 36 min [29]. Furthermore, there is no curing process through the vitrification mechanism during the quenching process in the gelation phase state [35].

The decrease in crosslink to about 50% occurred in the three-time quenching at a temperature of 150°C. At glass transition temperature, some segments of the epoxy resin chain become free to move due to the increase in volume because of expansion. In this condition, there is an opportunity for the epoxy chain to undergo rearrangement if sufficient time is available. However, the quenching pro-cess at a fast cooling rate results in insufficient time for the epoxy resin to rearrange [12]. The effect of rapid cooling also does not allow the epoxy resin to reach an equilibrium condition, so the atoms that make up the polymer chain cannot adjust their position to fill the vacant space during
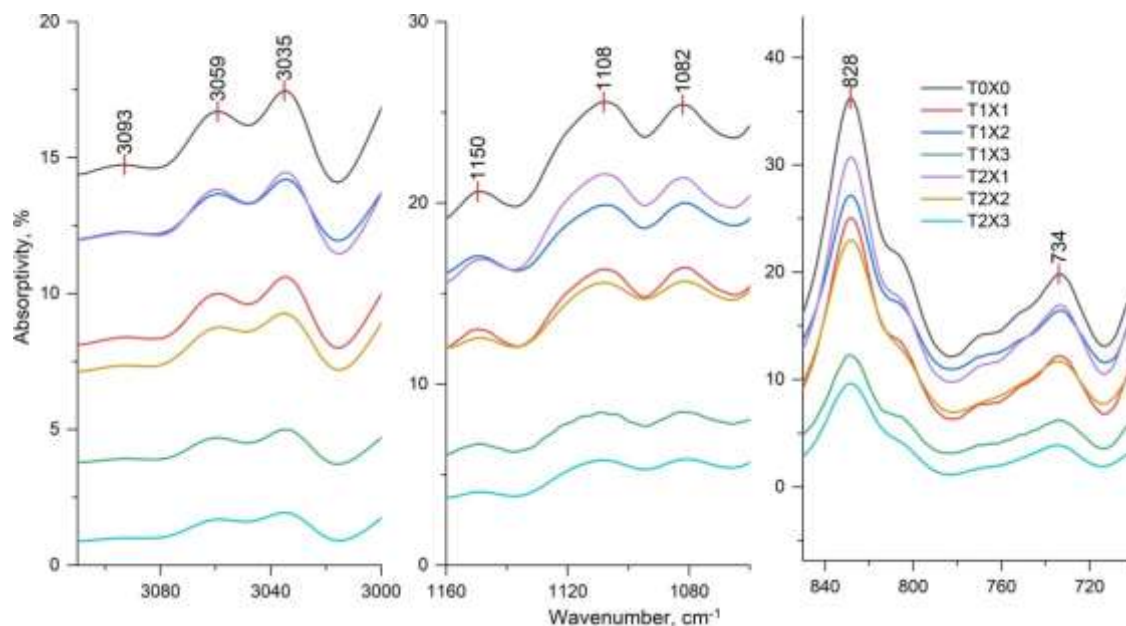
Figure 5: Infrared peaks area of specimen for crosslink conversion calculation.

Table 4: Calculation of function group conversion of epoxy resin

Specimen	Peak area, 10^{-18} cm^2/mol		R_{ij}	Peak area, 10^{-18} cm^2/mol		R_{ij}
	A_f at 3,059/ cm	A_r at 1,109/ cm		A_f at 828/ cm	A_r at 733/cm	
T0X0	2.597	4.961	1.000	8.226	5.123	1.000
T1X1	1.471	2.894	0.971	4.049	2.896	1.148
T1X2	2.003	3.977	0.962	6.301	4.413	1.125
T1X3	0.672	1.497	0.858	2.386	0.852	0.573
T2X1	2.01	4.14	0.927	6.59	4.23	1.031
T2X2	1.289	2.852	0.863	4.933	2.856	0.930
T2X3	0.215	0.965	0.426	1.79	0.6325	0.567

heating [36]. In addition, when the epoxy resin is heated to approximately the glass transition temperature, it may experience a thermo-mechanical effect due to the poly- mer's softening or decomposition. More critical degrada-
tion is possible when the material is heated in an oxidizing environment or free air rather than in a vacuum or inert gas [37]. This degradation due to heating is related to the
weight reduction of the epoxy resin, which at each surface depth has a different degradation rate [38]. This surface degradation can potentially increase water absorption when the epoxy resin is subjected to a quenching process. The
presence of water in the resin will degrade the thermome-chanical properties, adhesion, and chemical degradation of the polymer network and crosslinks and damage the

dimensions due to swelling. When absorbed in an epoxy resin, water is found in the form of free water molecules, which are highly mobile ($\approx$3,600/cm) and water moleculesbonded by hydrogen bonds ($\approx$3,300/cm) [30].

Tensile strength of epoxy resin

The stress–strain curve from the tensile test indicates that the epoxy resin has brittle properties. The yield area that usually appears in ductile materials does not appear in the tensile test yield curve, as shown in Figure 6a. The brittle nature is also shown on macroscopic photos in the form of fracture lines of the test specimen in the fracture shapes that do not show yield areas, strain hardening and necking, as usually occurs in ductile materials, which is shown in Figure 6b. The single quenching treatment of theepoxy resin at a target temperature of 125°C showed a significant decrease in strain and stress that can represent

tensile strength, reaching 46 and 27%, respectively, com-pared to the epoxy resin without quenching. Repeated quenching at 125°C increased tensile strength and strain or elongation, although it did not reach the strength of unquenched epoxy resin but decreased the fracture mod-ulus, as indicated in Table 5. However, repeated quenching at 150°C reduces tensile strength but increases the modulus. The portion of strain reduction that is greater than the stressreduction results in an increase in fracture modulus (stress/
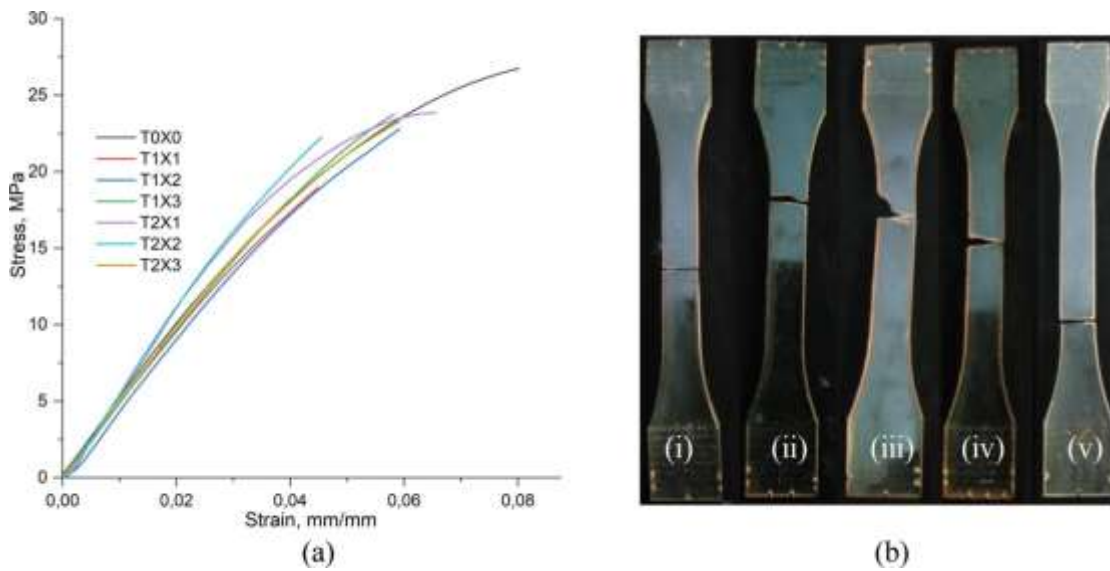strain) calculation, even though the tensile strength is

Figure 6: (a) Stress to strain curve and (b) tensile fracture patterns of epoxy resin specimen: (i) T0X0, (ii) T1X2, (iii) T2X2, (iv) T1X3, and (v) T2X1.

Table 5: Stress and strain of epoxy resin after quenching treatment

Specimen	Stress (MPa)		Strain (mm/mm)		Modulus of fracture (MPa)
	Mean	CV (%)	Mean	CV (%)	
T0X0	26.463	3	0.081	4	326.704
T1X1	19.282	4	0.044	4	438.227
T1X2	23.367	5	0.056	8	417.268
T1X3	23.444	4	0.061	4	384.328
T2X1	23.958	4	0.071	10	337.437
T2X2	21.831	5	0.055	7	396.927
T2X3	21.558	5	0.050	9	431.160

reduced. In this case, the epoxy resin with a higher modulus will be obtained at the lower tensile strength and *vice versa*. The heating stage during the quenching process in an atmospheric environment allows oxidation of the epoxy resin. The oxidation is generally characterized by the disappearance of the hydroxyl group and generating a carbonyl compound as a carboxylate group. An infrared spectrum detects this group at a wavenumber of 1,550—1,610/cm [39]. Epoxy resins with conditions above the glass transition temperature will generally experience an uncontrolled reaction because oxygen will easily and quickly diffuse into the epoxy [40]. In addition, the molecular oxide as the product of the cleavage of the primary polymer chains or the breaking of crosslinks has properties as volatile. It is trapped on the surface of the epoxy resin [41]. In addition, the non-equilibrium state of the epoxy resin causes the

formation of a glassy state that takes place continuously around T_g so that the epoxy properties will be affected when cooling occurs around it. Generally, glass formation makes epoxy materials stiffer and more brittle [42].

Furthermore, the oxidation of adjacent hydroxyl groups forms an ether chain. Oxidation of hydroxyl also causes intra-molecular dehydration in the epoxy resin, which further oxidizes to form a carboxylate group [43]. Therefore, the presence of hydroxyl groups may be increased on repeated quenching treatment. The mobility of the epoxy resin molecules when heated and followed by immersion in water provides an opportunity for the addition of hydroxyl groups because there is sufficient energy for water molecules to diffuse into the epoxy resin [44]. The dispersed water molecules can then more easily access other polar groups which have less energy or which have low enthalpy values [45]. The hydroxyl group can be attributed to the epoxy resin's thermal degradation and oxidation, which is dominated by the weakest atomic bond [46].

Interlaminar shear strength (ILSS) of composite CFRP

Changes in stress and strain of epoxy resin after quenching treatment are not correlated commensurately with changes in the ILSS value of CFRP composite. The short beam bending test shows an increase in the ILSS of the composite after quenching. The increase in the three-point flexural load applied during the test and displacement did not
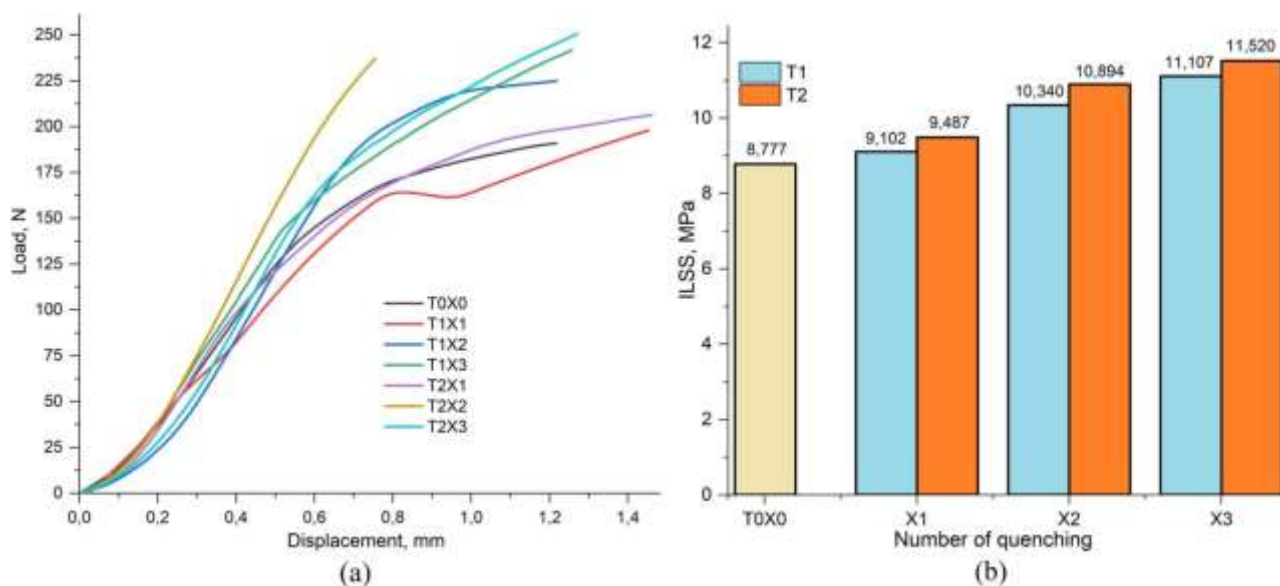
Figure 7: (a) Load to displacement curves result from short beam bending test of CFRP composite and (b) the ILSS comparison afterquenching treatments.

show the same pattern for all quenching treatments, as shown in the curve in Figure 7a. However, a higher target temperature and repeated quenching increased ILSS with a relatively constant gradient, as shown in Figure 7b. The maximum increase was obtained in the quenching treatment three times at a target temperature of 150°C, which was 31% of the ILSS value of the composite without quenching, as shown in Table 6. The maximum statistical CV value is 18%, which means that the standard deviation of the data is still within acceptable limits [47].

Thermal loading has the potential to provide significant chemical and structural changes to the epoxy resin crosslink network as well as reduced CO_2 content. These changes affect the mechanical properties of epoxy as an adhesive, coating, or composite matrix [48]. Interfacial reactions can also provide different morphological modifications to the epoxy microstructure around the fibersurface. Carbon fiber and epoxy resin's complex interfacial structure region entangles various physical interactive forces, such as hydrogen bonding, van der Waals, electrostatic interactions, or mechanical interlocking [49]. The interaction between carbon fiber and matrix during thermal treatment is essential because, around this location, the matrix material

is migrated to the interfacial zone with low molecular mobi-lity. The resulting microstructural gradient can promote crackinitiation and propagation through this region [50]. In addition, the thermal shock causes internal thermal stress due to the expansion and contraction of the material during heating and cooling or due to differences in the coefficient of thermal expansion of the composite material components [9]. Epoxy resins also undergo dimensional deviation when heated and cooled at the same rate [10]. In CFRP composites, carbon fiber and polymer matrices significantly differ in thermal expansion coefficient. Microscopically, they also have the potential to cause internal interfacial stresses due to differences in the rate of deformation when subjected to thermal loads [12]. The deformation rate differences between the carbon fiber and the epoxy resin lead to the crosslink breakdown and the formation of stress concentrations at the inter-face. In the case of the quenching cycle, the repeated heating and cooling processes affect the tensile and impact strengths of the CFRP composite for two reasons. First is the difference in the coefficient of thermal expansion of carbon fiber and epoxy, which forms deformation, micro-crack, and stress concentration in the interface area. The second is post-curing, which potentially occurs at high temperatures,

Table 6: The ILSS between carbon fiber mat and epoxy resin

Specimen	T0X0	T1X1	T1X2	T1X3	T2X1	T2X2	T2X3
ILSS (MPa)	8.777	9.102	10.340	11.107	9.487	10.894	11.520
CV (%)	17	17	18	18	16	15	17

increases the crosslinks chain in the interface region and improves the ILSS [14]. As a consequence, the epoxy resin may form an interpenetrating network. It is also possible for the epoxy molecules of one surface to diffuse fast into the other, which may result in more excellent inter-diffusion bonding [51]. The increased ILSS may also be enhanced by the improved thermo-mechanical performance attributed to the interfacial covalent interactions engendered by the ring-opening reaction between the epoxy and the amine moi- eties [52].

5 Discussion

Epoxy resins experience two crucial phenomena during the quenching process. The first is forming a carboxylic group from the hydroxyl oxide, which helps improve the epoxy resin's strength. Second, a thermo-mechanics effect due to rapid cooling reduces the epoxy resin strength. The quenching treatment dominates the destructive impact on the tensile strength of the epoxy resin because there is not enough time for the epoxy resin to set a balanced arrangement during heating. Meanwhile, the presence of carboxylate in the CFRP composite bridges the carbon fiber surface and the epoxy resin. This bridge demonstrates that a stoichiometric chemical bonding is formed between

these carboxylic groups and the diamine hardener [53], which will be faster by epoxy resin heating. Two opposing mechanisms occur when the CFRP composite is heated, namely, post-curing contributing to improving ILSS and interfacial deformation between the fiber surface and the epoxy resin resulting in a decrease in ILSS. The dominant one between the two will play a role in determining the ILSS. The phenomena of epoxy resin ductility and the inter-laminar shear strength after quenching are depicted in Figure 7. The unquenched sample (Figure 8a) shows a crack in the resin in linear propagation, leading per- pendicularly to the carbon fiber. Then, the crack bends following the interface between the epoxy resin and the carbon fiber. This damage model shows the ductility of the epoxy resin and the weakness of ILSS. The contra- dictory fact is seen in the sample with three times quenching at a temperature of 150°C (T2X3). A higher ILSS is proven by the fracture model reaching and damaging the carbon fiber, and the brittle epoxy resin produces a wider fracture opening than just a single fracture line (Figure 8(b)).

In the building industry, epoxy resins are commonly used for roofing, flooring, and cementing [54]. The roof system is a layer that resists the flow of liquid damage to the walls or roof structure. Furthermore, a rubber compound is usually prepared in which the epoxy resin is enhanced with the necessary additives for making a sheet roof.
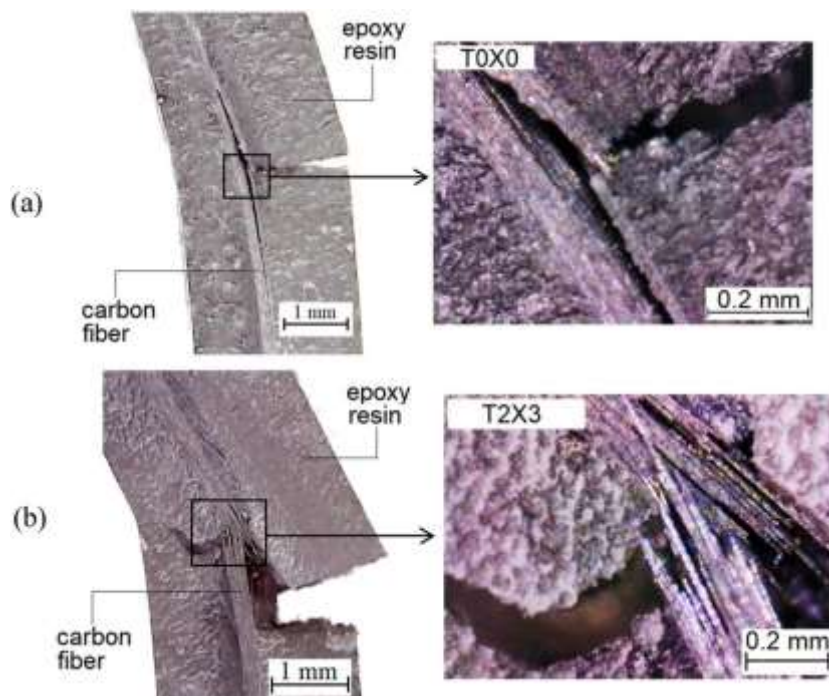

Figure 8: Macroscopic images of fracture pattern of (a) T0X0 and (b) T2X3 samples.

This sheet is applied to the roof in the cured state. The advantage of this sheet is that its large size, up to 15 m wide, can remove the required seams and joints [55]. However, applications such as roofing have the consequence of exposure of the epoxy resin to harsh conditions that cause deterioration of properties over a period. Damage can occur due to strong winds, sun exposure, rainfall, yielding, and temperature changes [56]. On the other hand, thermosetting epoxy resins resistant to heavy traffic, abrasion, chemical or water spills, and intensive cleaning make them also often used for flooring. Epoxy resin formulations in cement or concrete, referred to as synthetic resin flooring, are applied to improve their properties ranging from increased strength to underwater durability and to obtain high-performance flooring systems [57].

The use of high-performance materials such as CFRP for structures has been applied to replace concrete-based materials. It permits a drastic reduction in self-weight and allows for the design of lightweight structural ele- ments. One application is the T-beam member, the com- posite CFRP used as a reinforcement for high-performance concrete. The CFRP T-beam is stiffer than the beams without reinforcement, but the deflections were allowed to be comparatively large. However, delamination failure occurred during the tensile tests of the T-beam, leading to the concrete cover spalling [58]. Reducing the weight of structural components by using CFRP composites is also used for bridge construction. The most existing develop- ment in the last 20 years has been the design and con- struction of a composite bridge which will make it possible to build a bridge with a span longer than that possible with steel and concrete. A bridge made with traditional mate- rials collapses under its weight when its length exceeds about 1,950 m. The dynamic loads on the bridge also con- tribute to fatigue failure in its construction. To overcome this problem, the brittle nature of CFRP, which is dan- gerous when subjected to fluctuating loads, is anticipated by adding an elastomer in the form of a latex emulsion to the bridge structure material. The resulting composites have a higher flexural strength and lower water perme- ability [59].

Although ILSS composites do not degrade under quenching, the fact that the ductility of the cycloaliphatic amine-cured epoxy resin is reduced should be a concern for engineers to apply to constructions with dynamic loads or walls that are directly exposed to weather changes [60]. The oxidation layer on the epoxy resin's surface can potentially reduce the strain-at-break by two types of sur- face behavior: voiding and cracking [61]. Brittle materials are more susceptible to rapid crack propagation when an initial crack is exposed to dynamic loads than ductile

materials [62]. In addition, cracks in the epoxy resin matrix impact the penetration of oxygen and moisture directly into the reinforcing fiber, so in a relatively short period, it will reduce the performance of the reinforcing fiber in the composite.

6 Conclusion

The cycloaliphatic amines cured DGEBA epoxy resin has T_g of 131°C at fully consolidated condition. When sub- jected to quenching treatment up to three times at tem- peratures of 125 and 150°C, this epoxy resin showed a higher percentage of strain reduction than stress reduc- tion, referring to this material without quenching. It is due to the domination of the thermo-mechanic effect compared to the formation of carboxyl during the quenching process. However, the quenching treatments improved ILSS when this epoxy resin was used as a matrix in CFRP composites. The diffusivity of the epoxy resin molecules at high tem- peratures allows them to diffuse into the pores between the carbon fibers to form a strong bond or mechanical interlocking.

However, in terms of future needs that might drive innovations, one has to develop easy methods of recy- cling thermosets and composites that have reached the end of their useful lives. Reducing the strength and elon- gation or ductility of epoxy resins can be used to create new surfaces on CFRP composite easily. A slight bending has the potential to generate a lot of cracks in the epoxy resin without damaging the carbon fiber. This crack is an opportunity that can be used to accelerate the degrada- tion of epoxy resin by chemical reactions in the context of after-used CFRP composites recycling. The solvolysis method is an attractive alternative allowing suitable che- mical solutions to directly penetrate the composite inter-facial surface through the already-formed cracks [63]. The large contact surface can potentially increase the rate of chemical reactions so that improving the perfor- mance of the solvolysis process in recycling can be rea- lized [64].

of research methods and discussions of ILSS. Dody Ariawan is a supervisor and polymer expert, contributed to the discussion and analysis of FTIR and XRD data. Joko Triyono is a supervisor in data processing, contributed to statistical data analysis of tensile load and short beam bending tests.

Conflict of interest: The authors state no conflict of interest.

References

[1] Frohs W, Jaeger H. Carbon fiber & composite material - land-scape Germany. SGL Carbon. 2012;50(2):737.

[2] Sloan J. Carbon fiber 2007 looks forward with optimism. Carbon Fibers. 2008;16(1):1–4.

[3] Huang X. Fabrication and properties of carbon fibers. Materials (Basel). 2009;2(4):2369–403.

[4] Roberts A. The carbon fibre industry worldwide 2008-2014. Innov Text. 2009;4:1–11.

[5] Ratna D, Simon G. Thermal and mechanical properties of a hydroxyl-functional dendritic hyperbranched polymer and tri-functional epoxy resin blends. Poly Eng Sci. 2001;41(10):1815–22.

[6] Shechter L, Wynstra J, Kurkjy RP. Glycidyl ether reactions with amines. Ind Eng Chem. 1956;48(1):94–7.

[7] Patel P, Lucas P, Dibiase J. Cycloaliphatic amines for epoxy formulation: A novel curing agent for epoxy systems. PCT/EP2019/055237; 2019.

[8] Smith A, Krass PE, William F. Process for reducing cure time in cycloalphatic amne based epoxy resens. US005414067A; 1995.

[9] King D, Bell JP. Thermal shock failure in thick epoxy coatings. J Adhes. 1988;26(1):37–58.

[10] Ahmed A, Tavakol B, Das R, Joven R, Roozbehjavan P, Minaie B. Study of thermal expansion in carbon fiber-reinforced polymer composites. In: Bechwith SW, editor. SAMPE International Symposium Proceedings; 2012 Oct 22–25; Charleston (SC), USA. SAMPE, 2012. p. 1–13.

[11] Yu B, Kodur V. Effect of temperature on strength and stiffness properties of near-surface mounted FRP reinforcement. Compos Part B Eng. 2014;58:510–7.

[12] Papanicolaou GC, Xepapadaki AG, Tagaris GD. Effect of thermal shock cycling on the creep behavior of glass-epoxy composites. Compos Struct. 2009;88(3):436–42.

[13] Ray BC. Effect of thermal shock on interlaminar strength of thermally aged glass fiber-reinforced epoxy composites. J Appl Polym Sci. 2006;100(3):2062–6.

[14] Shishevan AF, Akbulut H, Mohtadi-Bonab MA. The effect of thermal shock cycling on low velocity impact behavior of carbon fiber reinforced epoxy composites. J Dyn Behav Mater. 2019;5(2):161–9.

[15] Changsheng C, Yuan L, Hongyin C, Weiqi H. Method for preparing 3-aminomethyl-3,5,5-trimethylcyclohexylamine. CN101386579B; 2008.

[16] Suryanto H, Marsyahyo E, Surya Irawan Y, Soenoko R. Aminudin. improvement of interfacial shear strength of mendong fiber (fimbristylis globulosa) reinforced epoxy com-posite using the AC electric fields. Int J Polym Sci. 2015;2015:1–10.

[17] Sukanto H, Raharjo WW, Ariawan D, Triyono J. Temperature Quenching Effect on Tensile Strength of DGEBA Cured Cycloaliphatic Hardener. In: Abdollah MF, Amiruddin H, Singh ASP, Munir FA, Ibrahim A, editors. 7th International Conference and Exhibition on Sustainable Energy and Advanced Materials; Nov 2021; Melaka, Malaysia. Springer,2021. p. 73–7.

[18] Nandiyanto ABD, Oktiani R, Ragadhita R. How to read and interpret ftir spectroscope of organic material. Indones J Sci Technol. 2019;4(1):97–118.

[19] Maity P, Kasisomayajula SV, Parameswaran V, Basu S, Gupta N. Improvement in surface degradation properties of polymer composites due to pre-processed nanometric alumina fillers. IEEE Trans Dielectr Electr Insul. 2008;15(1):63–72.

[20] Coates J. Interpretation of infrared spectra, a practical approach. Anal Chem. 2000;12:10815–37.

[21] American Society for Testing and Materials. ASTM D638-14, standard test method for tensile properties of plastics. West Conshohocken (PA), USA: ASTM International. 2014;82(C):1–15.

[22] ASTM D2344. Standard test method for short-beam strength of polymer matrix composite materials and their laminates. West Conshohocken (PA), USA: ASTM International. 2003;3(2):136–40.

[23] Rahmatpanah Z, Alavi Nikje MM. A novel synthesis of poly-butadiene-based polyurethane binder and conductive gra- phene–polyurethane nanocomposites: A new approach to polybutadiene recycling. Polym Bull. 2021;78(7):3651–66.

[24] Nagaraj SK, Shivanna S, Subramani NK. Revisiting powder X-Ray diffraction technique: A powerful tool to characterize polymers and their composite films. J Mater Sci. 2016;4(4):1–5.

[25] Paajanen A, Vaari J, Verho T. Crystallization of cross-linked polyethylene by molecular dynamics simulation. Polymer (Guildf). 2019;171:80–6.

[26] Sook C, Sung P. Fluorescence and IR characterization of epoxy cured with aliphatic amines. Polymer. 2005;46:9378–84.

[27] Smith B. Infrared Spectral Interpretation: A Sytematic Approach. Boca Raton (FL): CRC Press Taylor & Francis; 1998.p. 135–40.

[28] Wu C, Xu W. Atomistic molecular modelling of crosslinked epoxy resin. Polymer. 2006;47:6004–9.

[29] Simon S, Gillham J. Thermosetting cure diagrams: Calculation and application. Appl Polym Sci. 1994;53:709–27.

[30] Gonzáles M, Cabanelas JC, Baselga J. Application of FTIR on epoxy resin - identification, monitoring the curing process, phase separation and water uptake. In: Theophile T, editor. Infrared Spectroscopy-Materials Science, Engineering and Technology. London: InTech; 2012. p. 2610–84.

[31] Nikolic G, Zlatkovic S, Cakic M, Cakic S, Lacnjevac C, Rajic Z. Fast fourier transform IR characterization of epoxy GY systems crosslinked with aliphatic and cycloaliphatic EH polyamine adducts. Sensors. 2010;10(1):684–96.

[32] Tran TN, Mauro CDi, Graillot A, Mija A. Monitoring the struc- ture-reactivity relationship in epoxidized perilla and safflower oil thermosetting resins. Polym Chem. 2020;11(31):5088–97.

[33] Fouchal F, Dickens P. Monitoring the polymerization of a diglycidyl ether bisphenol-a/2,2′-dimethyl-4,4′-methylenebis

(cyclohexylamine) matrix with a fourier transform infrared optical fibre sensor. Proceedings of the Institution of Mechanical Engineers, Part L: Journal of Materials: Design and Applications. Sage; 2004;218(4):331–44.

[34] Pandita SD, Wang L, Mahendran RS, MacHavaram VR, Irfan MS, Harris D, et al. Simultaneous DSC-FTIR spectroscopy: Comparison of cross-linking kinetics of an epoxy/amine resin system. Thermochim Acta. 2012;543:9–17.

[35] Gillham JK. The time temperature transformation (TTT) state diagram and cure. In: Seferis JC, Nicolais L, editor. The role of the polymeric matrix in the processing and structural proper-ties composite materials. London: Plenum Press; 1983.
p. 127–45.

[36] Oliveira BF, Creus GJ. An analytical-numerical framework for the study of ageing in fibre reinforced polymer composites. Compos Struct. 2004;65(3–4):443–57.

[37] Tsotsis TK. Thermo-oxidative aging of composite materials.
J Compos Mater. 1995;29(3):410–22.

[38] Hancox NL. Thermal effects on polymer matrix composites:
Part 2. Thermal degradation. Mater Des. 1998;19:93–7.

[39] Heacock R, Marion L. THE infrared spectra of secondary amines and their salts. Can J Chem. 1956;4141:1782–95.

[40] Awad SA, Fellows CM, Saeed Mahini S. A comparative study of accelerated weathering of epoxy resins based on DGEBA and HDGEBA. J Polym Res. 2018;25(4):102–10.

[41] Mailhot B, Morlat-Thérias S, Ouahioune M, Gardette JL. Study of the degradation of an epoxy/amine resin, 1 photo- and thermo-chemical mechanisms. Macromol Chem Phys. 2005;206(5):575–84.

[42] Kong ES-W. Physical aging in epoxy matrices and composites. Epoxy resins and composites IV. Advances in polymer science. Berlin, Heidelberg: Springer; 1986. p. 125–71.

[43] Park W, Blount J. Oxidative degradation of epoxy resin coat-ings. Ind Eng Chem. 1957;49(11):1897–902.

[44] Gibhardt D, Buggisch C, Meyer D, Fiedler B. Hygrothermal aging history of amine-epoxy resin: Effect on thermo-mechanical properties. Front Mater. 2022;9(82):60–76.

[45] Elkebir Y, Trinh D, Trinh D. Effect of physical ageing onto the water uptake in epoxy coating. Electrochim Acta. 2020;20:1–24.

[46] Wolfrum J, Eibl S, Lietch L. Rapid evaluation of long-term thermal degradation of carbon fibre epoxy composites. Compos Sci Technol. 2009;69(3–4):523–30.

[47] Romano FL, Ambrosano GMB, Magnani MBB, de A Nouer DF. Analysis of the coefficient of variation in shear and tensile bond strength tests. J Appl Oral Sci. 2005;13(3):243–6.

[48] Bockenheimer C, Fata D, Possart W. New aspects of aging in epoxy networks: Thermal aging. J Appl Polym Sci. 2004;91(1):361–8.

[49] Jamshaid F, Khan RU, Islam A. Performance improvement of glass fiber/epoxy composites upon integrating with

[50] N-(2-aminoethyl)-3-aminopropyltrimethoxysilane functiona-lized graphene oxide. J Inorg Organomet Polym Mater. 2021;31(9):3810–22.

[50] Sharpe LH. The Interphase in adhesion†. J Adhes. 1972;4(1):51–64.

[51] Fiore V, Valenza A. Epoxy resins as a matrix material in advanced fiber reinforced polymer composites. In: Bai J, editor. Advanced fibre-reinforced polymer (FRP) composites for structural appli- cations. Cambridge: Woodhead Publishing Ltd; 2013. p. 88–121.

[52] Jamshaid F, Khan RU, Islam A. Performance tuning of glass fiber/epoxy composites through interfacial modification upon integrating with dendrimer functionalized graphene oxide.
J Appl Polym Sci. 2021;138(35):1–13.

[53] Fitzer E, Geigl KH, Hüttner W, Weiss R. Chemical interactions between the carbon fibre surface and epoxy resins. Carbon. 1980;18(6):389–93.

[54] Agarwal S, Gupta RK. The use of thermosets in the building and construction industry. Oxford: Elsevier Ltd; 2018. p. 279–302.

[55] GangaRao H. Infrastructure applications of fiber-reinforced polymer composites. Oxford: Elsevier Inc; 2011. p. 565–84.

[56] Berdahl P, Akbari H, Levinson R, Miller WA. Weathering of roofing materials - an overview. Constr Build Mater. 2008;22(4):423–33.

[57] Ohama Y. Recent progress in concrete-polymer composites. Adv Cem Based Mater. 1997;5(2):31–40.

[58] Kromoser B, Preinstorfer P, Kollegger J. Building lightweight structures with carbon-fiber-reinforced polymer-reinforced ultra-high-performance concrete: Research approach, con- struction materials, and conceptual design of three building components. Struct Concr. 2019;20(2):730–44.

[59] Fowler DW. Polymers in concrete: A vision for the 21st century. Cem Concr Compos. 1999;21(5–6):449–52.

[60] Astakhov VP. Mechanical properties of engineering materials: Relevance in design and manufacturing. In: Davim JP, editor. Introduction to Mechanical Engineering. New York (NY), USA: Springer International Publishing; 2018. p. 3–41.

[61] Wei XF, Kallio KJ, Bruder S, Bellander M, Kausch HH, Gedde UW, et al. Diffusion-limited oxidation of polyamide: Three stages of fracture behavior. Polym Degrad Stab. 2018;154:73–83.

[62] Beaumont PWR, Young RJ. Failure of brittle polymers by slow crack growth - part 1 crack propagation in polymethylmetha-crylate and time-to-failure predictions. J Mater Sci. 1975;10(8):1334–42.

[63] Sukanto H, Raharjo WW, Ariawan D, Triyono J, Kaavesina M. Epoxy resins thermosetting for mechanical engineering. OpenEng. 2021;11(1):797–814.

[64] Ma Y, Nutt S. Chemical treatment for recycling of amine/epoxy composites at atmospheric pressure. Polym Degrad Stab. 2018;153:307–17.